

# New evidence of light-induced structural changes detected in As–S glasses by photon energy dependent Raman spectroscopy

R. Holomb<sup>a,\*</sup>, N. Mateleshko<sup>a</sup>, V. Mitsa<sup>a</sup>, P. Johansson<sup>b</sup>, A. Matic<sup>b</sup>, M. Veres<sup>c</sup>

<sup>a</sup> *Uzhhorod National University, Research Institute of Solid State Physics and Chemistry, 54 Voloshyn str., Uzhhorod 88000, Ukraine*

<sup>b</sup> *Department of Applied Physics, Chalmers University of Technology, Göteborg 41296, Sweden*

<sup>c</sup> *Research Institute for Solid State Physics and Optics, Department of Laser Applications, Budapest, Hungary*

Available online 20 March 2006

## Abstract

Light-induced structural changes of  $g\text{-As}_{40}\text{S}_{60}$  and  $g\text{-As}_{45}\text{S}_{55}$  were probed by macro FT-Raman and photon-energy dependent micro-Raman spectroscopy. We hypothesize that some new observed features in the Raman spectra of these glasses are related to transformations of  $\text{As}_4\text{S}_4$  molecules possible through the  $m\text{-As}_4\text{S}_4$  intermediate. At the same time, other processes, connected mainly with the layers, composed of pyramidal  $\text{AsS}_3$  structural units, take place. These new observed Raman modes and their possible interconnection to changes of the glassy structure are discussed.

© 2006 Elsevier B.V. All rights reserved.

PACS: 61.43.Fs; 61.46.+w; 78.30.-j

Keywords: Amorphous semiconductors; III–V Semiconductors; Raman scattering; Chalcogenides; Optical spectroscopy; Raman spectroscopy; Medium-range-order; Short-range-order

## 1. Introduction

Theoretical and experimental investigations in the last years have shown that chalcogenide glassy semiconductors (ChGS) continuous media are formed in a wider variety of basic short range order structural units (s.u.) than their crystalline analogs [1]. The majority are grouped into the medium-range ordering (MRO) grouping (clusters), depending on the concentration of additives and fabrication technology [2,3] used. The ordering groups geometry in the ChGS system's bulk glasses and films determine their physical properties [3]. During the past few years, a great importance has been assigned to structural fluctuations and separated nano-scale phases with homopolar As–As bonds in the interpretation of photo-induced phenomena in binary As–S glasses [4]. The concentration of nano-phases,  $C_{n.f.} \sim 1.0\text{--}2.0\%$  in  $g\text{-As}_2\text{S}_3$  is much larger than that

of charged defects ( $C_{\text{def}} \sim 1$  ppm) which is foreseen by modeling [5,6]. The charged defects model [5,6] for glasses has been known for a long time and it has been the most widely used one to explain the photo-induced absorption of ChGS. This model is also used to explain the optical behavior in ChGS induced by light with photon energies ( $E_i$ ) lower than the Tauc band gap ( $E_0$ ) in the Urbach edge region of optical absorption spectra.

In this article, micro- and macro FT-Raman spectroscopy have been used to examine of light-induced structural changes in stoichiometric and arsenic-rich As–S glass compositions.

## 2. Experimental details

The glasses of As–S binary system were synthesized by melt quenching from 873 K and a cooling rate of 1 K/s.

FT-Raman spectra were measured using a Bruker IFS 66 interferometer equipped with CCD detector and coupled to a Bruker FRA 106 Raman module. The near-IR

\* Corresponding author. Tel.: +38 031 33020.

E-mail address: [holomb@ukr.net](mailto:holomb@ukr.net) (R. Holomb).

Nd:YAG laser with wavelength of 1064 nm ( $E_1 = 1.17$  eV) was used as excitation source. The laser sources used for micro-Raman scattering excitation in As–S glasses were as follows: (i) a diode laser (785 nm,  $E_2 = 1.58$  eV), (ii) a He–Ne laser (632.8 nm,  $E_3 = 1.96$  eV) and (iii) an Ar-ion laser (514.5 nm,  $E_4 = 2.41$  eV). All measurements were performed at room temperature in back-scattering geometry. During recording of the micro-Raman spectra, the laser beams were focused by means of the 50 $\times$  objective of an optical microscope into a spot of diameter  $\sim 2$   $\mu\text{m}$  on the samples. Optical filters, limiting the output power to as low as 80  $\mu\text{W}$ , were used. The excitation time during recording of the micro-Raman spectra was limited to 60 s. For all micro-Raman measurements the estimated intensity on the sample was  $P \sim 10^3$   $\text{W}/\text{cm}^2$ .

### 3. Results

Spectral changes of the Raman spectra depending on the wavelength of exciting radiation for g-As<sub>45</sub>S<sub>55</sub> were recently described in [7]. In the same way, the very similar to g-As<sub>45</sub>S<sub>55</sub> (Fig. 1) spectral changes have also been observed in the Raman spectra of stoichiometric glass composition g-As<sub>40</sub>S<sub>60</sub> (Fig. 2).

As it is seen in Figs. 1(a) and 2(a) while exciting the FT-Raman spectrum with the photon energy of  $E_1 < E_0/2$ , the availability of bands at 187, 220 and 230  $\text{cm}^{-1}$  is common for both spectra. The intensity of these bands in FT-Raman spectra is higher for g-As<sub>45</sub>S<sub>55</sub> composition. Within the spectral region ranging from 300 to 400  $\text{cm}^{-1}$ , the split (342 and 360  $\text{cm}^{-1}$ ) wide band is characteristic for FT-Raman spectrum of g-As<sub>45</sub>S<sub>55</sub>, whereas the spectrum of

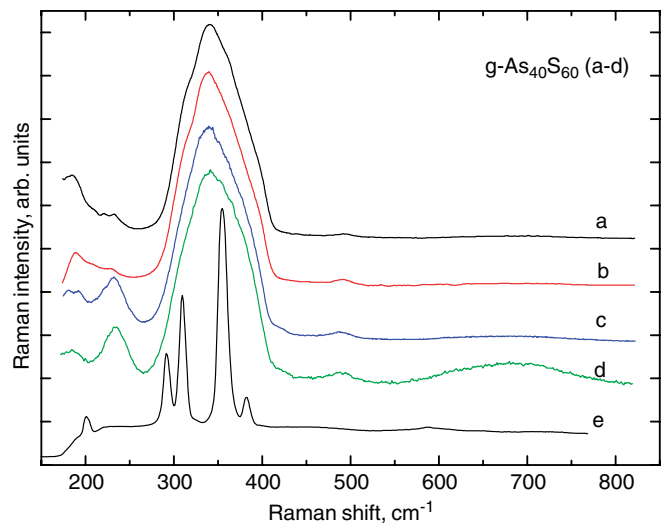


Fig. 2. FT-Raman spectrum of g-As<sub>40</sub>S<sub>60</sub> excited with photon energy of  $E_1 = 1.17$  eV (a) and micro-Raman spectra of the same sample excited with photon energies:  $E_2 = 1.58$  eV (b),  $E_3 = 1.96$  eV (c) and  $E_4 = 2.41$  eV (d). The micro-Raman spectra of polycrystalline As<sub>2</sub>S<sub>3</sub> is shown below for comparison (e).

g-As<sub>40</sub>S<sub>60</sub> comprises a typical wide maximum at 340  $\text{cm}^{-1}$  with shoulders at 310, 360 and 380  $\text{cm}^{-1}$ .

For both compositions at the sub-band illumination with  $E_2 = 1.56$  eV in micro-Raman spectra the visible redistribution of band intensities at 187 and 230  $\text{cm}^{-1}$  occurred (Figs. 1(b) and 2(b)). With increasing photon energy used for excitation to  $E_3$  the band intensity at 230  $\text{cm}^{-1}$  increases stepwise, but that of the one at 187  $\text{cm}^{-1}$  decreases. At  $E_4$ , the band intensity at 230  $\text{cm}^{-1}$  is maximal for both glasses. Furthermore, the half-width of the main complex band near 340  $\text{cm}^{-1}$  of g-As<sub>40</sub>S<sub>60</sub> increases with increasing photon energy used for excitation (Fig. 2(b)–(d)). The very similar behavior was observed in the photon energy dependent micro-Raman spectra of arsenic-excess As–S glass (Fig. 1(b)–(d)). At  $E_4$ , the new shoulder near 420  $\text{cm}^{-1}$  appears in high-frequency side of the most intensive band, and within the region of two-phonon Raman scattering of both glasses the intensity of vibrations near 680  $\text{cm}^{-1}$  becomes considerably larger. The differential (in comparison with FT-Raman spectra) Raman spectra (Fig. 3) clearly illustrate the changes in the intensity of new bands with increasing exciting photon energy  $E_i$ . The positions of maxima in these spectra for both compositions are given in Table 1. Ultimately, Fig. 3 clearly shows that the increase in the half-width of a complex band at 342  $\text{cm}^{-1}$  is due to the increase in band intensities near 300, 320 and 380  $\text{cm}^{-1}$ .

### 4. Discussions

#### 4.1. Polymorph transition and resonance Raman effect

In accordance with first-principle calculations of vibrational spectra of realgar (r) and para-realgar (p) types of

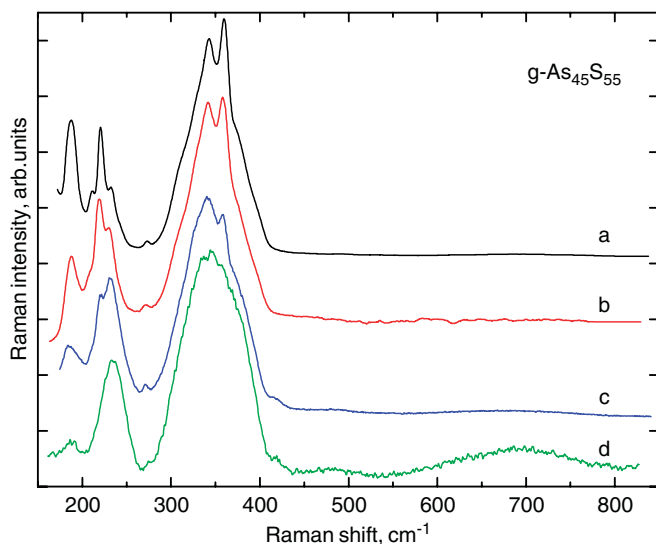


Fig. 1. FT-Raman spectrum of g-As<sub>45</sub>S<sub>55</sub> excited with photon energy of  $E_1 = 1.17$  eV (a) and micro-Raman spectra of the same sample excited with photon energies:  $E_2 = 1.58$  eV (b),  $E_3 = 1.96$  eV (c), and  $E_4 = 2.41$  eV (d).

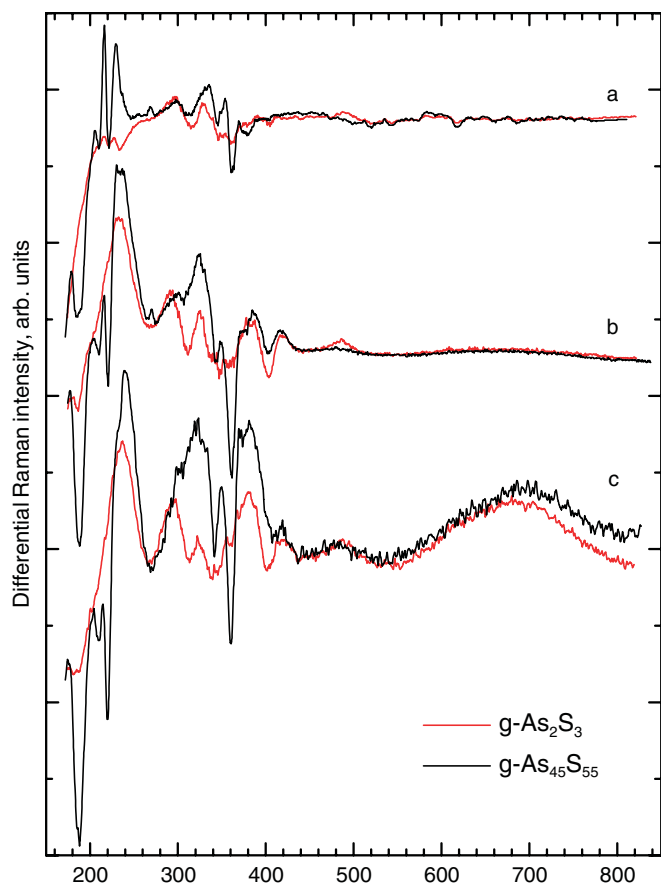


Fig. 3. Differential Raman spectra of  $g\text{-As}_{40}\text{S}_{60}$  and  $g\text{-As}_{45}\text{S}_{55}$  (compared to FT-Raman): (a)  $I^R(E_2) I^R(E_1)$ , (b)  $I^R(E_3) I^R(E_1)$ , (c)  $I^R(E_4) I^R(E_1)$ . All spectra were normalized to main band at  $340\text{ cm}^{-1}$  before subtracting.

Table 1

New Raman peaks ( $\text{cm}^{-1}$ ) observed in the differential Raman spectra of  $g\text{-As}_2\text{S}_3$  and  $g\text{-As}_{45}\text{S}_{55}$  (Fig. 3) with increasing exciting photon energy

Excitation photon energy, eV					
1.58 ( $E_2$ )		1.96 ( $E_3$ )		2.41 ( $E_4$ )	
$g\text{-As}_2\text{S}_3$	$g\text{-As}_{45}\text{S}_{55}$	$g\text{-As}_2\text{S}_3$	$g\text{-As}_{45}\text{S}_{55}$	$g\text{-As}_2\text{S}_3$	$g\text{-As}_{45}\text{S}_{55}$
			204		
	216		216		
	230	233	230–237	237	230(sh)–240
	269		270		
297	298	293	300	294	300
330	330–336	326	325	323	323
	348		349		349
	354			355	
		382	374–386	367–380	370–382
		~420	~418	~420	~419
~490		~487		~490	~483
		~665	~665	~685	~695

$\text{As}_4\text{S}_4$  molecules [7], the intensive vibration modes in the FT-Raman spectrum of  $g\text{-As}_{45}\text{S}_{55}$  at 187, 342 and  $360\text{ cm}^{-1}$  (Fig. 1(a)) may be assigned to valence vibrations of  $r\text{-As}_4\text{S}_4$  molecules. It is considered that  $\beta\text{-As}_4\text{S}_4$  microcrystals are implanted into  $g\text{-As}_{45}\text{S}_{55}$  amorphous matrix [8,9]. The part of  $\beta\text{-As}_4\text{S}_4$  nano-phase inclusions into

$g\text{-As}_{40}\text{S}_{60}$  does not exceed 2% and depend on the preparation condition [3,10]. Therefore, the band intensity at  $187\text{ cm}^{-1}$  for this composition is considerably lower. High-frequency valence vibrations of small quantity  $\beta\text{-As}_4\text{S}_4$  in FT-Raman spectrum of  $g\text{-As}_{40}\text{S}_{60}$  overlap by dominating the valence vibrations of  $\text{AsS}_{3/2}$  s.u. with the maximum at  $340\text{ cm}^{-1}$  (Fig. 2(a)). When excitation photon energy increases, the character of transformation of micro-Raman spectra for both stoichiometric and As-rich As–S glass compositions are very similar (Figs. 1(b)–(d) and 2(b)–(d)). Therefore the redistribution of band intensity at 187 and  $230\text{ cm}^{-1}$  may be assigned to the light-induced transformation of As–As bonds in  $r\text{-As}_4\text{S}_4$  molecule into As–As bonds of  $p\text{-As}_4\text{S}_4$  molecule. The decrease in the band intensity characteristic for  $\beta\text{-As}_4\text{S}_4$  at 187, 220, 342 and  $362\text{ cm}^{-1}$  is accompanied by the simultaneous growth in the bands intensities at  $\sim 230\text{--}239$ ,  $\sim 330\text{--}336$  and  $349\text{ cm}^{-1}$ . The last bands are connected with valence vibrations of  $p\text{-As}_4\text{S}_4$  molecule [7] and most clearly seen in the differential Raman spectra of As-rich As–S glass composition (Fig. 3). The calculations show that the appearance of a new band in micro-Raman spectra of both compositions at  $\sim 419\text{ cm}^{-1}$  (Figs. 1(c),(d) and 2(c),(d)) can be assigned to As–S vibrations of metastable (m)  $m\text{-As}_4\text{S}_4$  molecule. Such a molecule may be intermediate when one of the As–As bond is broken in  $\beta\text{-As}_4\text{S}_4$  molecule during structural transformations into the pararealgar  $\text{As}_4\text{S}_4$ . Charge transfer between atoms of this molecule change both the atomic force constants and electronic structure (MO energies) and results in shifting of vibration frequency and decreasing experimental band-gap of the material (known as photo-darkening). The detailed results of this calculation will be discussed independently. In addition, it should be noted that with increasing photon energy the band intensity at  $490\text{ cm}^{-1}$ , assigned to S–S bond, increases in the Raman spectra of  $g\text{-As}_{40}\text{S}_{60}$  (Figs. 2 and 3). The increasing of this peak was detected in the Raman spectra of  $g\text{-As}_{45}\text{S}_{55}$  when exciting photon energy of 2.41 eV was used (Fig. 1(d)).

From another point of view at  $E_2 = 1.96\text{ eV}$ , which is smaller than the threshold energy  $E_{\text{thres}} > 2\text{ eV}$  of the beginning of the intensive structural transformation of  $\beta\text{-As}_4\text{S}_4$  into  $p\text{-As}_4\text{S}_4$ , an unexpected great growth of the vibration mode at  $230\text{ cm}^{-1}$  does not exclude the superposition of resonance Raman effect of As–As bonds onto that of structural transformation. The resonance was observed in macro-Raman spectra of As–S glasses at  $E_2 = 2.41\text{ eV}$  [11]. The authors ascribed the  $230\text{ cm}^{-1}$  band to the resonance of As–As network bonds. Moreover, the observed considerable increase in the second order  $2\nu = 680\text{ cm}^{-1}$  scattering intensity at  $E_4$  (Figs. 1(d) and 2(d)) in micro-Raman spectra of both samples is known in molecular systems as the resonance Raman effect [12]. At  $E_4 = E_0$  the effect of increase in two-phonon ( $2\nu$ ) vibrations may be assigned to the resonant scattering with As–S bonds participating. Therefore, the transformation of the band near  $230\text{ cm}^{-1}$  with increasing photon energy can be connected

with two processes – resonance of As–As network bonds and alteration of realgar  $\text{As}_4\text{S}_4$  molecules to pararealgar form.

#### 4.2. Structural transformation

As can be seen by comparison of the differential Raman spectra of  $\text{g-As}_2\text{S}_3$  and  $\text{g-As}_{45}\text{S}_{55}$  (Fig. 3) except for the mentioned photo-induced transformation of  $\text{As}_4\text{S}_4$  molecules and/or possible resonance Raman effect, some other additional photo-induced effects take place. Undoubtedly, the observed features in the spectral region ranging from 290 to  $400\text{ cm}^{-1}$  are very complex. With increasing excitation photon-energy, the widening of the main complex band in the Raman spectra of both  $\text{g-As}_{45}\text{S}_{55}$  and  $\text{g-As}_{40}\text{S}_{60}$  occurs due to increase in the intensity of bands near 300, 320, 355,  $380\text{ cm}^{-1}$  (Fig. 3, Table 1). The common nature of these features for both glass compositions indicates that changes may occur in pyramidal-like structures. The Raman modes at about 300 and  $380\text{ cm}^{-1}$  are typical for polycrystalline (p)  $\text{p-As}_2\text{S}_3$  vibration modes at 292–310 and  $382\text{ cm}^{-1}$ , respectively (Fig. 2(e)). Furthermore, at  $E_4$  the shape of  $\text{g-As}_{45}\text{S}_{55}$  micro-Raman spectrum is close to that of  $\text{g-As}_{40}\text{S}_{60}$  spectrum (Figs. 1(d) and 2(d)). Focused laser beam causes heating of the irradiated area of the glassy material. An abnormal growth of the first sharp diffraction peak in As–S glasses was observed with increasing temperature [13]. The temperature studies (from room temperature to above  $T_g$ ) of X-ray structure factor of  $\text{As}_x\text{S}_{100-x}$  glasses have revealed increase in the first sharp diffraction peak intensity with increasing temperature, while the second diffraction peak intensity normally decreased. The author connected this phenomenon with the layering effect. One can suppose that at the intensities of laser radiation ( $P \sim 10^3\text{ W/cm}^2$ ) used and a high level of absorption ( $\alpha_4(E_4) \sim 5 \times 10^4\text{ cm}^{-1}$ ) in the radiation zone of samples, the temperature can increase. However, the quantitative aspect of this supposition requires additional research. On the other hand, our calculation showed that the photon-energy dependence ( $E_2$ – $E_4$ ) of peak positions which causes the widening of the main maximum may be connected with the change of the geometrical parameters of  $\text{AsS}_3$  pyramids (apex angles) and angles between them. First-principle calculations (DFT/BLYP/6-311 G\*) show that both symmetric (Raman active) and asymmetric (IR active) modes of  $\text{AsS}_3$  s.u. can shift in frequency with changes of the S–As–S angle. For Raman mode the frequency shifts from 334 to  $330\text{ cm}^{-1}$  with increasing the apex angle from 90 to 100 degree ( $^\circ$ ). At apex angle of  $110^\circ$ , this peak shifts to  $311\text{ cm}^{-1}$ . Also, it is important to note that between  $100$ – $110^\circ$  there are frequency transpositions of IR and Raman modes – Raman mode has lower frequency than IR mode. With further increase S–As–S of the apex angle ( $120^\circ$ ) for planar  $\text{AsS}_3$  model these features disappear and frequency of  $324\text{ cm}^{-1}$  was calculated for Raman mode. Therefore, the features near 300 and  $320\text{ cm}^{-1}$  in the differential Raman

spectra of both glasses (Fig. 3) may indicate two states of  $\text{AsS}_3$  pyramid apex angles. As can be seen from Fig. 3, the intensity of  $\sim 320\text{ cm}^{-1}$  Raman mode is higher for As-rich As–S glass composition and the intensity of this mode increases with increasing exciting photon energy (1.58, 1.96, and 2.41 eV) that may be connected with light-induced planarity of the network. The maximum at  $380\text{ cm}^{-1}$  is assigned to As–S–As water-like vibrations [14]. The exciting photon energies also influence the intensity of this peak in the differential Raman spectra of both As–S glasses. For both compositions there exist a peculiarity at about  $370\text{ cm}^{-1}$  which is very intensive at the exciting photon energy of 2.41 eV.

#### 5. Conclusions

We have used macro FT-Raman and photon energy dependent micro-Raman spectroscopy for investigation of light-induced features in stoichiometric ( $\text{As}_{40}\text{S}_{60}$ ) and arsenic-excess ( $\text{As}_{45}\text{S}_{55}$ ) glass compositions. It was observed that the spectral evolution of micro-Raman spectra of  $\text{As}_{40}\text{S}_{60}$  and  $\text{As}_{45}\text{S}_{55}$  glass compositions excited with different photon energies are connected with two light-induced transformation effects. The first one is an alteration of beta realgar-like  $\text{As}_4\text{S}_4$  molecules embedded in the glass network and more obviously observed for As-excess  $\text{As}_x\text{S}_{100-x}$  glass. The second one, common for both glass compositions, is an effect connected with the changes of geometrical parameters of layer-like structures. The broadening of the main band ( $\sim 340\text{ cm}^{-1}$ ) in the micro-Raman spectra of both glasses with increase in photon energy used for excitation is related to the formation of new Raman modes near 300, 320, and  $380\text{ cm}^{-1}$ . At exciting photon energies close to Tauc's band-gap (2.41 eV), the growth of intensity of two-phonon scattering intensity, typical for resonance Raman in molecular systems, was detected.

#### Acknowledgements

One of us (R.H.) is grateful to the Swedish Institute for scholarship support. We would also like to thank Professor A. Stronski for many helpful discussions.

This work was supported in part by the Ministry of Education and Science of Ukraine (Grant Nos. M/467-2003 and DB-507) and by Hungarian-Ukrainian Intergovernmental S&T (Project No. UKR-12/2004).

#### References

- [1] R.M. Holomb, V.M. Mitsa, J. Optoelect. Adv. Mater. 6 (2004) 1177.
- [2] S.I. Simdyankin, S.R. Elliott, Phys. Rev. B 69 (2004) 144202.
- [3] V. Mitsa, Doctoral thesis, Institute of Semiconductors Physics, NAS of Ukraine, Kyiv (2003).
- [4] K. Petkov, J. Optoelect. Adv. Mater. 4 (2002) 611.
- [5] A.V. Kolobov (Ed.), Photo-Induced Metastability in Amorphous Semiconductors, Wiley-VCH, Weinheim, 2003.
- [6] M. Kastner, D. Adler, H. Fritzsche, Phys. Rev. Lett. 37 (1976) 1504.
- [7] R. Holomb, V. Mitsa, P. Johansson, N. Mateleshko, A. Matic, M. Veresh, Chalcogenide Lett. 7 (2005) 63.

- [8] P.J.S. Ewen, M.J. Sik, A.E. Owen, *Solid State Commun.* 33 (1980) 1067.
- [9] D.G. Georgiev, P. Boolchand, *Philos. Mag.* 83 (2003) 2941.
- [10] F. Kosek, J. Chlebny, Z. Cimple, J. Mašek, *Philos. Mag. B* 47 (1983) 627.
- [11] P.J.S. Ewen, A.E. Owen, *J. Non-Cryst. Solids* 35&36 (1980) 1191.
- [12] A. Weber (Ed.), *Raman Spectroscopy of Gases and Liquids*, Springer-Verlag, Berlin, Heidelberg, New York, 1979.
- [13] L.E. Busse, *Phys. Rev. B* 29 (1984) 3639.
- [14] R.J. Kobliska, S.A. Solin, *Phys. Rev. B* 8 (1973) 756.